

Final Draft
of the original manuscript:

Nadutov, V.M.; Kosintsev, S.G.; Svystunov, Y.O.; Haramus, V.M.;
Willumeit, R.; Eckerlebe, H.; Ericsson, T.; Annersten, H.:

Anti-Invar properties and magnetic order in fcc Fe–Ni–C alloy

In: Journal of Magnetism and Magnetic Materials (2011) Elsevier

DOI: 10.1016/j.jmmm.2011.05.053

Anti-Invar Properties and Magnetic Order in FCC Fe-Ni-C Alloy

V. M. Nadutov^a, S. G. Kosintsev^a, Ye. O. Svystunov^a, V. M. Garamus^b,
R. Willumeit^b, H. Eckerlebe^b, T. Ericsson^c, S.G., H. Annersten^c

^a*G.V. Kurdyumov Institute for Metal Physics of the N.A.S. of Ukraine, Kyiv, Ukraine*

^b*Helmholtz-Zentrum Geesthacht: Zentrum für Material- und Küstenforschung GmbH, Geesthacht, Germany*

^c*Uppsala University, Uppsala, Sweden*

Abstract. Anti-Invar effect was revealed in the f.c.c.-Fe-25.3%Ni-0.73%C (wt%) alloy, which demonstrates high values of thermal expansion coefficient (TEC) (15 - 21) 10^{-6} K^{-1} accompanied by almost temperature-insensitive behavior in temperature range of 122 K – 525 K. Alloying with carbon considerably expanded the low temperature range of anti-Invar behaviour in f.c.c. Fe-Ni-based alloy. Measurements of temperature dependences of magnetic susceptibility and saturation magnetization allowed to determine the Curie temperature of the alloy $T_C = 195 \text{ K}$. The Mössbauer and small-angle neutron scattering (SANS) experiments on the f.c.c.-Fe-25.3%Ni-(0,73-0,78)%C alloys in the varying temperature range 150-293 K and in external magnetic field of 1,5 – 5 T were conducted. Low value of the Debye temperature $\Theta_D = 180 \text{ K}$ was estimated using the temperature dependence of the integral intensity of Mössbauer spectra for specified temperature range. The inequality $B_{\text{eff}} = (0.7 \div 0.9)B_{\text{ext}}$ was obtained in Mössbauer measurement applying external magnetic field that points to antiferromagnetically coupled Fe atoms, which have a tendency to align their spins perpendicular to B_{ext} . Nano-length-scale magnetic inhomogeneities nearby and far above T_C were revealed, which supposedly caused by mixed antiferromagnetically and ferromagnetically coupled Fe atom spins. The anti-Invar behavior of Fe-Ni-C alloy is explained in terms of evolution of magnetic order with changing temperature resulting from thermally varied interspin interaction and decreasing stiffness of interatomic bond.

Keywords: Fe-Ni-C, Anti-Invar, Thermal expansion, Curie point, Mössbauer spectra, SANS
PACS: 75.25.-j; 75.50.Bb; 75.75.-c; 76.80.+y.

INTRODUCTION

The enhanced thermal expansion coefficient (TEC) of the order of $\alpha = (20-25) \cdot 10^{-6} \text{ K}^{-1}$, which is weakly changed with the elevating temperature above the martensitic point, is observed in γ -Fe and the f.c.c. binary Fe-(10-25)%Ni alloys [1, 2]. Observed TEC value of the Fe-(10-25)%Ni alloys significantly exceeds TEC for pure elements Fe ($13.2 \cdot 10^{-6}$ at 400 K) and Ni ($13.7 \cdot 10^{-6}$ at 400 K) [3]. Despite the high TEC values is common to the f.c.c. metals and alloys the described Fe-Ni alloys demonstrate deviation of TEC temperature dependence from the well known Grüneisen behavior remaining almost constant over wide temperature range. Such behavior is described as anti-Invar effect [1, 2] and considered as high temperature property in contrast to the Invar effect, which predominantly occurs below the Curie point [4].

To describe the anti-Invar behavior occurring in γ -Fe, f.c.c. Fe-Ni and Fe-Ni-Mn alloys far above magnetic ordering temperature the phenomenological two-level

system formalism was proposed [1, 2], which was based on the Weiss's two γ Fe-state model [5] assuming an existence of low-volume low-spin antiferromagnetic (LS AF) phase as ground state separated from energetically higher-lying large-volume high-spin ferromagnetic (HS FM) state. [6]. An existence of LS AF and the HS FM states has been verified by Mössbauer measurements on γ -Fe precipitates in Cu and Cu-Al [7]. With increasing temperature, a change of a population of the one state at the expense of another state determines the anti-Invar behavior. However, the data derived from monochromatic circularly polarized Mössbauer analysis of $\text{Fe}_{1-x}\text{Ni}_x$ ($x = 0,25, 0,30, 0,35$) alloys [8] were in contradiction with described two γ -state model.

On the other hand the anti-Invar effect ($\alpha = 50 \cdot 10^{-6} \text{ K}^{-1}$) is most clearly found in YMn_2 compounds and explained as a result of thermal evolution of the amplitude of spin fluctuations in paramagnetic temperature range above the Neel temperature T_N [9]. Such an approach was introduced to explanation of thermal anomalies in Fe-Ni-systems [10].

Considerable effect of alloying Fe-Ni alloys with carbon on the Curie point, magnetic ordering and γ -phase thermal stability [11, 12] is well known and may provide exhibition of anti-Invar TEC behavior in alloys such as γ -Fe-(20-25)%Ni-C. In case of spin fluctuations model is right, the magnetic SANS intensity and Mössbauer line broadening in the vicinity and higher T_C is expected.

In order to establish the mechanism of anti-Invar behavior occurring below and above the Curie point the main purpose of this work was to reveal changes in magnetic order in the γ -Fe-25%Ni-C alloy at varying temperature and the effect of applied external magnetic field on magnetic state.

EXPERIMENTAL

The Fe-25.3%Ni-(0.73-0.78)%C alloys were melted in a vacuum induction furnace in protective argon atmosphere. The cast material was annealed at 1273 K for 3 hrs. The C concentration was determined by chemical analysis and the Ni content was obtained by means of X-ray fluorescence analysis.

The temperature dependences of TEC were obtained on automated quartz dilatometer [11] within the temperature range of 120 – 530 K. The initial length of a sample was measured with the accuracy of $\pm 0,005$ mm. The experimental curves were smoothed and the TEC values were calculated automatically with the accuracy $\pm 0,3 \cdot 10^{-6} \text{ K}^{-1}$.

The Curie point of the alloys was determined by measurement of the temperature dependence of ac magnetic susceptibility within the temperature range of 77–330 K. The magnitude of magnetic field and the frequency were $400 \text{ A} \cdot \text{m}^{-1}$ and 1 kHz, respectively. Thermal dependence of saturation magnetization in constant magnetic field 800 kA m^{-1} was measured using ballistic magnetometer within the temperature range 77-400 K.

The Mössbauer spectra were measured on a constant acceleration spectrometers MS1101E at the G.V. Kurdyumov Institute for Metal Physics of N.A.S. of Ukraine and on the Uppsala University spectrometer in Sweden. The $^{57}\text{Co}(\text{Cr})$ and $^{57}\text{Co}(\text{Rh})$ matrix were used as gamma quantum sources. A Cryogenic Ltd. closed cycle

refrigerator superconducting magnet with a central field homogeneity of 99 % was used for in field measurements. Low temperature measurements were conducted using specially constructed cryostat [13]. The applied longitudinal magnetic field was parallel to the gamma beam. The spectra were stored in a multichannel scaler with 512 channels. All spectra were fitted using Window's analysis and standard discrete method.

SANS experiments were performed at the SANS-1 and SANS-2 instruments at the FRG-1 research reactor of GKSS [14]. The neutron wavelength was 8.5 Å and the wavelength resolution was 10%. The range of scattering vectors on SANS-1 $0.05 < q < 2.5 \text{ nm}^{-1}$ was obtained using four sample-to-detector distances (SDD): 0.7, 1.1, 3.8, 9.7 m. For SANS-2 the range of scattering vectors $0.05 < q < 2.5 \text{ nm}^{-1}$ was obtained using three SDD's: 1.17, 3.92, 9.92 m. The neutron beam and applied magnetic field perpendicular to the neutron beam were used. Some measurements have been done on polarized neutron beam with the initial polarization close to 1, while the efficiency of the spin flipper to realize the inverse polarization state was 0.9.

All samples were annealed at 1373 K in vacuum during 30 min and subsequently quenched in oil and the X-ray analysis (Co^α radiation) controlled the phase content.

RESULTS

Structure and properties. The X-ray analysis has shown that annealed samples of the Fe-25.3%Ni-0.73%C alloy were in austenitic state (Fig. 1) with the lattice parameter of austenite of $a_\gamma = 0.3602 \text{ nm}$ which correlates with the effect of carbon on the lattice expansion [15].

Slow rise in saturation magnetization as temperature falls points to increasing in close magnetic ordering (Fig. 2, a). According to this measurement martensitic transition occurs at 118 K and results in dramatic increase of saturation magnetization value below that point.

Temperature dependence of magnetic susceptibility shows that there is transition to ferromagnetically ordered state at 195 K (Fig. 2, b). According to $\chi(T)$ dependence martensitic point was $M_S = 122 \text{ K}$ i.e. phase transition occurs in magnetically ordered state. It is established that phase transition results in rise of sample temperature on ~25 K.

Therefore thermomagnetic curves demonstrate significant changes in the alloy magnetic order, which have to affect anti-Invar thermal expansion anomaly that is believed to be of magnetic nature.

The dilatometric measurements have shown that the TEC of the Fe-25.3%Ni-0.73%C alloy is abnormally high $15\text{--}21 \cdot 10^{-6} \text{ K}^{-1}$ within the temperature range 122 K–525 K (Fig. 2, c). The values of α are approximately twice as higher than that for pure α -Fe and γ -Ni and are consistent with TEC of high-temperature γ -Fe and f.c.c.-Fe-(10-25)%Ni phases [1, 2]. The TEC is accompanied by almost temperature-insensitive behaviour in interval 300 – 525 K and it slowly decreases below room temperature (Fig. 2, c). Thus the Fe-25.3%Ni-0.73%C alloy shows anti-Invar behavior below and above the Curie point that is consistent with the data obtained for the f.c.c. Fe-Ni-C alloys with lower carbon concentrations [16]. It is opposite to Invar effect in the Fe-

30%Ni-C alloy, which shows abnormally low thermal expansion ($\sim 2 \cdot 10^{-6} \text{ K}^{-1}$) that is observed solely in magnetically ordered state below the Curie point [11, 12].

Notice, that in contrast to statement [1] the anti-Invar behaviour is not just a high-temperature property (that is attributed in γ -Fe and the Fe-Ni alloys [1, 2]) due to alloying with carbon and it is observed below and above the magnetic transition point (Fig. 2, c).

The probable reason of the anti-Invar behavior in the Fe-Ni-C alloy with the change of temperature from high value below the Curie point is moment-volume instability in magnetic order [17]. The magnetic order evolution is based on the Kondorski and Sedov idea about mixed exchange interactions in Fe-Ni system between atomic spins of Fe and Ni [18], the earlier Weiss model [5] and energy calculations [6] concerning an existence of different LS AF and HS FM states with the thermally induced population. In order to reveal changes in magnetic order with the temperature the Mössbauer and SANS measurements at low temperatures 150-295 K and under external magnetic field were conducted.

Mössbauer effect in anti-Invar Fe-Ni-C alloy. Mössbauer spectrum of the Fe-25.3%Ni-0.73%C alloy at room temperature consists of broadened singlet s that is attributed to Fe atoms having only Fe and Ni atoms as the nearest-neighbors (nn) and doublet d caused by electric quadruple hyperfine interaction relating to Fe atoms with mainly Fe and C atoms as the nn (Fig. 3, *a*). As shown in [19] observed singlet broadening have magnetic nature. Inhomogeneous close atomic order in Fe-Ni-C austenite considered as a result of increasing thermodynamical activity of carbon in Fe-Ni solid solution by Ni. Thus, the magnetically broadened singlet s was fit with sextet with the small hyperfine field $B_s = 0.72 \text{ T}$ as it was proposed in [19]. The quadruple splitting and isomer shift of these components are $\delta_s = -0.034 \text{ mm/s}$; $\delta_d = 0.009 \text{ mm/s}$; $\Delta = 0.673 \text{ mm/s}$ respectively. The obtained parameters correspond to those for Fe-Ni-C austenite with close chemical composition [19].

Mössbauer measurements show gradual broadening spectra line with the decreasing temperature from 295 K to 248 K, 198 K and 163 K (Fig. 3). The doublet d resulting from hyperfine quadruple interaction vanishes and transforms gradually in smeared quasicontinual singlet. The hyperfine magnetic fields (HMF) distribution shows their gradual increase under the cooling above and below $T_C = 195 \text{ K}$ in the temperature interval from 295 K to 163 K that points to changes in magnetic state.

The decrease of the Mössbauer spectrum integral intensity I with the increasing temperature in specified temperature range from 163 K to 295 K and especially its drastically reduction with the large slope below T_C was observed (Fig. 2 *c*) that attributed to decreasing recoil-free fraction f . The Debye temperature that is measure of the interatomic bond stiffness was estimated using the temperature dependence $f(T)$ in the Debye model [20, 21]. The obtained low value of $\Theta_D = 180 \text{ K}$ for specified temperature range points to weakening stiffness of interatomic bond which can be responsible for large TEC values of anti-Invar alloys nearby the Curie point.

Fig. 4 shows Mössbauer spectra of the Fe-25.3%Ni-0.78%C alloy derived under external longitudinal magnetic field (EMF) of 2.5 T and 5 T (parallel to gamma beam). It was established that EMF causes broadening of the spectra lines (Fig. 4, *a*) increasing HMF (Fig. 4, *b*).

Moreover, HMF grows more slowly than EMF ($B_{\text{eff}} = (0.7 \div 0.9)B_{\text{ext}}$). Similar behavior of HMF under the B_{ext} was also observed in mechanically alloyed f.c.c. Fe-(21-27)%Ni powders [22] and Invar Fe-30.5%Ni-1.5%C alloy [23]. It means that B_{ext} had induced a local magnetic moment, which gave rise to an induced hyperfine field that was opposite in direction to B_{ext} . According to Mössbauer data for Fe-Ni-C alloy measured in the field of 5 T [23, 24] the inequality between B_{eff} and B_{ext} means that Fe atoms, which antiferromagnetically coupled, have a tendency to align their spins perpendicular to B_{ext} . This supports Weiss idea that in Fe-Ni Invar alloy two phases or states do coexist.

SANS in anti-Invar Fe-Ni-C alloy. The SANS curves for the Fe-25.3%Ni-0.73%C alloy obtained at room temperature for $B_{\text{ext}} = 0$ and 1.5 T and 5 T are presented in Fig. 5 a.

The SANS intensity was averaged by φ -angle and summarized by spin direction in the Fe-25.3%Ni-0.73%C alloy. One can see that at scattering vector $q < 0.17 \text{ nm}^{-1}$ the applied magnetic field B_{ext} perpendicular to neutron beam did not change the SANS intensity that points to nuclei scattering from large-scale inhomogeneities with no magnetic contribution. The dramatically decreasing intensities of scattering at $q > 0.17 \text{ nm}^{-1}$ under the field of 1.5 T that is approximately 5 times as less is observed. The effect of B_{ext} on SANS in Invar Fe-30.5%Ni-1.5%C alloy was observed in whole interval of scattering vectors $0.05 < q < 2.5 \text{ nm}^{-1}$ [25]. This means that there is short-range inhomogeneous magnetic order in the Fe-25.3%Ni-0.73%C alloy above the Curie point, the state of which are sensitive to B_{ext} . Using a simple relationship $R = 1/q$ a maximal average linear size of the magnetic inhomogeneities 6 nm was estimated.

The size of the small length-scale aggregates has been estimated also using the Indirect Fourier Transformation (IFT) approach [26] with assumption of the trace contributions of large objects (smooth interface due to obtained slope $\alpha = 4$) and small nearly spherical objects. Obtained parameters of small aggregates: maximal size D_{max} , gyration radius of scattering length densities R_g and „forward scattering“ $I(0)$, which is connected with concentration, volume and scattering contrast of smaller aggregates as $I(0) = nV^2\Delta\rho^2 = \phi V\Delta\rho^2$) are listed in Table 1. Here n is concentration of aggregates, V is volume of aggregate, $\Delta\rho$ is neutron scattering contrast, ϕ is volume fraction of aggregates and $\phi = nV$. As it can be seen the applied magnetic field 1.5 T lets to decreasing of maximal size of aggregates from $D_{\text{max}}=5$ nm to 3.5 nm and corresponding radius of gyration decreases from $R_g = 1.5$ nm to 1.1 nm. It can be explained by disassemble (partial disassemble) of a magnetic domains which is confirmed by corresponding decreasing the value of parameter $I(0)$ from 0.17 to 0.05. If ϕ and $\Delta\rho^2$ are the same before and after applying magnetic field, $I(0)$ should be proportional to $V \sim R_g^3$ that we see in present case. We can suggest that magnetic domain become smaller but volume fraction of damains is the same.

| Table 1. The results of the anti-Invar Fe–25.3%Ni-0.73%C (wt. %) alloy SANS curves approximation. | | | | | | |
|---|-------------------------|-------------------------------|--------------------------------------|--------------------------|-----------------|-------------------|
| Treatment | H_{ext} , T | Spin polarization on/of | Power law exponent α | D_{max} , nm | R_g , nm | $I(0)$ |
| Annealing 1373 K, quenching in oil, (sample #2) | 0 | – | 4.0 ± 0.2 | 5 | 1.48 ± 0.02 | 0.17 ± 0.01 |
| | 1.5 | – | 4.0 ± 0.2 | 3.5 | 1.07 ± 0.02 | 0.049 ± 0.002 |
| | 1.5 | of (parallel spin) | 4.0 ± 0.2 | 3.5 | 1.10 ± 0.02 | 0.046 ± 0.002 |
| | 1.5 | on (antiparallel spin) | 4.0 ± 0.2 | 3.5 | 1.05 ± 0.02 | 0.052 ± 0.002 |
| Annealing 1373 K, quenching in oil (sample #1) | 0 | - | 4.0 ± 0.2 | 5 | 1.50 ± 0.02 | 0.17 ± 0.01 |
| Ageing 773 K (sample #1) | 0 | - | 4.0 ± 0.2 | 5 | 1.52 ± 0.02 | 0.18 ± 0.01 |
| | 1,5 | - | 4.0 ± 0.2 | 3.5 | 1.11 ± 0.02 | 0.050 ± 0.002 |

Thus the smaller length-scale aggregates of the magnetic nature in the Fe–25.3%Ni-0.73%C alloy can be imagined as approximately 10 unit cells clusters (domains). However, magnetically disordered state was not removed completely under the $B_{\text{ext}} = 1.5$ T and the smaller length-scale magnetic inhomogeneities are still existing far above the Curie point $T_C = 195$ K since the anisotropy of 2D scattering pattern at large q was still observed (Fig 4 a, insert).

In order to estimate smoothness of the inhomogeneities in the alloy all SANS data (Fig. 5) have been analyzed at low q interval ($q < 0.1 \text{ nm}^{-1}$) by power law dependence $d\Sigma(q)/d\Omega \sim q^\alpha$. At this small scattering vectors the value of exponent $\alpha = 4 \pm 0.2$ that attributed to the Porod law [16]. This means that SANS for small q interval results from the large length-scale inhomogeneities ($R > 1/q = 10 \text{ nm}$), which are characterized by smooth surfaces (interfaces). The scattering from these large length

scale aggregates was not affected by 1.5 T (Fig 4 *a*), that means these inhomogeneities have not been removed under B_{ext} . The scattering by them did not depend on spin polarization ON/OFF (Fig. 4 *b*). Moreover the applied magnetic field 1.5 T and spin polarization did not change the value of the exponent α (Table 1). All the data points to mainly nuclear contribution to the SANS at low q interval ($q < 0.017 \text{ nm}^{-1}$). One can assume these aggregates are inhomogeneous atomic microareas enriched with Fe-C bonds on one had and Fe-Ni bonds on another one. The existence of C-C pairs as the first nearest neighbors of Fe atoms and Ni nearest neighbors in the vicinity of Fe depleted with carbon in the Fe-25.3%Ni-0.49%C austenite was revealed in [19].

In order to remove smaller length-scale magnetic inhomogeneities existing in the alloy far above the Curie point and to reveal reaction of the large length-scale inhomogeneities on external magnetic field we try to increase B_{ext} . The increase of B_{ext} to 5 T enhanced the effect of field on SANS intensity mainly at large q by approximately 35 times and there was still no any changes at $q < 0.017 \text{ nm}^{-1}$ (Fig. 4 *c*) similarly to the effect of 1.5 T (Fig. 4 *a*). However, the anisotropy of scattering on 2D pattern obtained at large q was not observed at $B_{\text{ext}} = 5 \text{ T}$ that points to completely removing large length-scale inhomogeneities. Moreover the use of the polarized neutrons did not reveal any differences in SANS intensity at $B_{\text{ext}} = 5 \text{ T}$ (Fig. 4 *d*).

To characterize the evolution of the inhomogeneous magnetic order under cooling the SANS was measured above and below T_C and nearby T_C : at 250 K, 200 K, 150 K. The reduction of SANS intensity that could support the spin fluctuations model [9, 10] was not revealed. By contrast, the growth of scattering intensity in the range of large and middle q with decreasing temperature within interval 250 K - 200 K above the Curie point (195 K) was observed (Fig. 4 *e*). This points to gradual increase of maximal sizes of the magnetic inhomogeneities under the cooling approximately from 6 nm to 17 nm. Cooling to 150 K below T_C caused dramatic growth of SANS intensity predominantly in the range of small scattering vectors that points to the formation of the magnetic large length-scale inhomogeneities. One can assume the disoriented magnetic domains responsible for enhanced SANS intensity. If so such domains can be aligned in external magnetic field. In fact, the low temperature experiment under magnetic field of 5 T has shown the dramatic SANS intensity reduction in whole interval of scattering vectors (Fig. 4 *f*).

Thus the SANS experiment has shown an existence of the magnetic inhomogeneities in anti-Invar Fe-25.3%Ni-0.73%C alloy the sizes of which were varied from nanolength-scale magnetic inhomogeneities ($\leq 6 \text{ nm}$) above the Curie point to large length-scale magnetic domains below T_C ($> 17 \text{ nm}$).

In order to determine the effect of carbon on the formation of magnetic state of the Fe-25.3%Ni-0.73%C alloy we measured SANS after ageing of sample at 773 K for 2 hrs that we assumed should result in redistribution of atoms and graphitization. No considerable changes of SANS intensity due to ageing were observed within all interval of q . The SANS curves after annealing and ageing become just weakly separated at small q (Fig. 5 *a*). Moreover the effect of polarized beam on SANS intensity is similar to that observed for annealed sample (Fig. 4 *b*).

The analysis of SANS data by power law dependence $d\Sigma(q)/d\Omega \sim q^\alpha$ at low $q < 0.01 \text{ \AA}^{-1}$ gave the value of exponent α . The obtained α equals to 4 ± 0.2 (Table 1) and attributed to the Porod law [16] as previously for annealed sample and accordingly to

[16, 26] corresponds to large length-scale atomic inhomogeneities with smooth surfaces. The estimated parameters using the IFT approach [26] has shown that maximal size D_{\max} of small aggregates, radius gyration of scattering length densities R_g and the „forward scattering“ $I(0)$ are almost the same as compared to those of annealed sample (Table 1).

The dramatically decreasing SANS intensities at $q > 0.017 \text{ nm}^{-1}$ under 1.5 T was revealed for annealed sample (Fig. 5 b). The effect of external magnetic field on aged sample is similar to that revealed for sample after initial solution treatment (Fig. 4 a).

Thus the experiment with the ageing at 773 K has shown that there are small length-scale magnetic inhomogeneities in the Fe–25.3%Ni–0.73%C alloy, which did not depend on state of carbon in a solid solution and are determined by substitutional subsystem.

CONCLUSIONS

1. The anti-Invar effect is not just a high-temperature property attributed to pure γ -Fe and f.c.c. Fe-Ni alloys. Alloying with carbon (0,73 wt%) of Fe-Ni austenite provides display of anti-Invar behaviour: abnormally high $\langle\alpha\rangle = (15-21)\cdot 10^{-6} \text{ K}^{-1}$ above and below $T_C = 195 \text{ K}$ in the temperature range 122 K – 525 K.

2. Mössbauer experiment in the temperature range of 163 K - 295 K has shown a gradual change of hyperfine magnetic fields and the drastically reduction of integral spectra intensity nearby T_C that points to decreasing recoil-free fraction f at heating. The estimated Debye temperature using the temperature dependence of the integral spectra intensity for specified temperature range shows low value $\Theta_D = 180 \text{ K}$ that means small stiffness of interatomic bond in studied alloy.

It was established that external magnetic field B_{ext} increases hyperfine magnetic field B_{eff} therewith its growth behind the B_{ext} value. The obtained inequality $B_{\text{eff}} = (0.7\div 0.9)B_{\text{ext}}$ points to antiferromagnetically coupled Fe atoms, which have a tendency to align their spins perpendicular to B_{ext} .

3. SANS experiments in external magnetic field and at low temperatures have revealed inhomogeneous magnetic order in f.c.c. Fe–Ni–C alloy that implies nanolength-scale magnetic inhomogeneities of $\leq 6 \text{ nm}$ above the Curie point and of $> 17 \text{ nm}$ below T_C , which result from mixed antiferromagnetically and ferromagnetically coupled Fe spins and can be removed by $B_{\text{ext}} = 5 \text{ T}$.

4. The evolution of magnetic state with changing temperature resulting from thermally varied interspin interaction and decreasing stiffness of interatomic bond nearby T_C are responsible for anti-Invar behavior of the f.c.c. Fe-Ni-C alloy.

REFERENCES

1. M. Acet, T. Schneider, H. Zähres, E.F. Wassermann, W. Pepperhoff, *J. Appl. Phys.* 75, 10 (1994) 7015-7017.
2. M. Acet, H. Zähres, E.F. Wassermann, W. Pepperhoff, *Phys. Rev. B* 49 9 (1994) 6012.
3. S.I. Novikova, Thermal Expansion in Solids, Nauka, Moscow, 1974, p. 291. (In Russian)

4. Physics and Applications of Invar Alloys (Honda Memorial Series on Materials Science) 3, Tokyo: Maruzen Company Ltd., 1978, p. 646.
5. R.J. Weiss, Proc. Phys. Soc. 82 (1963) 281-288.
6. V.L. Moruzzi, P.M. Marcus, J. Kubler, Phys. Rev. B 39 (1989) 6957.
7. W. Keune, T. Ezawa, W.A.A. Macedo, et al., Physica B 161 (1989) 269.
8. D. Satula, K.Szymanski, L. Dobrzynsky, K. Rechko, J. Walishewski, Nukleonika, 48 (Suppl. 1) (2003) S71-S74.
9. M. Shiga, H. Wada, H. Nakamura, K. Yoshimura, Y. Nakamura, J. Phys. F 17 (1987) 1781-1793.
10. M. Shiga, Metals and Alloys. 1, 3 (1996) 340-348.
11. V.M. Nadutov., Ye.O. Svystunov, Metallofiz. Noveishie Tekhnol. 24, 12 (2002) 1639-1649. (In Ukrainian).
12. V.M. Nadutov., Ye.O. Svystunov, S.G. Kosintsev, O.I. Zaporozhets, V.A. Tatarenko, Izv. RAN, Seriya Fizicheskaya 69, 10 (2005) 1475-1481. (In Russian).
13. V.M.Nadutov., Ye.O.Svystunov, V.E. Isyanov, Pribory Techn. Experimenta 5 (2007) 165-167. (In Russian).
14. H.B. Stuhmann, N. Burkhardt, G. Dietrich, R. Jünemann, W. Meerwinck, M. Schmitt, J. Wadzack, R. Willumeit, J. Zhao, K.H. Nierhaus, Nucl. Instr. Meth. A356 (1995) 133.
15. V.M. Nadutov, S.G. Kosintsev, Ye.O. Svystunov, Metallofiz. Noveishie Tekhnol. 31, 11 (2009) 1479 - 1491.
16. G. Porod, Kolloid Z., 125 (1952) 51.
17. E.F. Wassermann, J. Magn. Magn. Mater. 100 (1991) 346.
18. E.I. Kondorsky, V.L. Sedov, JETP 38, 3 (1960) 773-779. (In Russian).
19. V.N. Bugaev, V.G. Gavriljuk, V.M. Nadutov, V.A. Tatarenko, Acta Metallurgica 31, 3 (1983) 407-418.
20. V.G Gavriljuk, V.M. Nadutov, FMM, 54, 5, (1982), 960 - 966.
21. G.K. Wertheim. Mössbauer effect: principles and applications. Academic Press, New York and London, 1964; Mir, Moscow, 1964, p. 172 .
22. Y.A. Abdu, H. Annersten, T. Ericsson, P. Nordblad, J. Magn. Magn. Mater. 280 (2004) 243-250.
23. V.M. Nadutov., T. Ericsson, S.G. Kosintsev, S.M. Bugaychuk, Ye.O. Svystunov H.Annersten, Hyperfine Inter. 168 (2006) 1023-1027.
24. U. Gonser, S. Nasu, W. Kappes, J. Magn. Magn. Mater. 10 (1979) 244-251.
25. V.M. Nadutov, V.M. Garamus, R. Willumeit, D.V.Semenov, Functional Materials 11, 3 (2004) 501-505.
26. J.S. Pedersen, Adv. Colloid Interface Sci. 70 (1997) 171

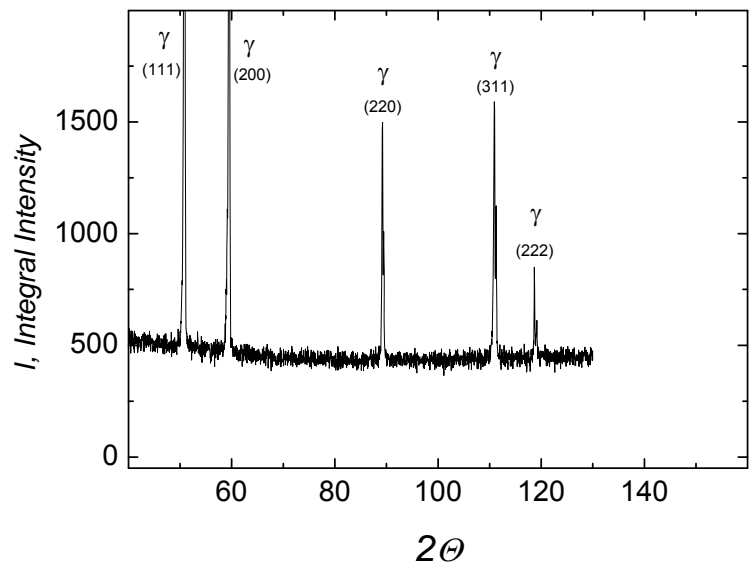


FIGURE 1. X-Ray diffraction pattern of Fe-25,3%Ni-0,73%C alloy

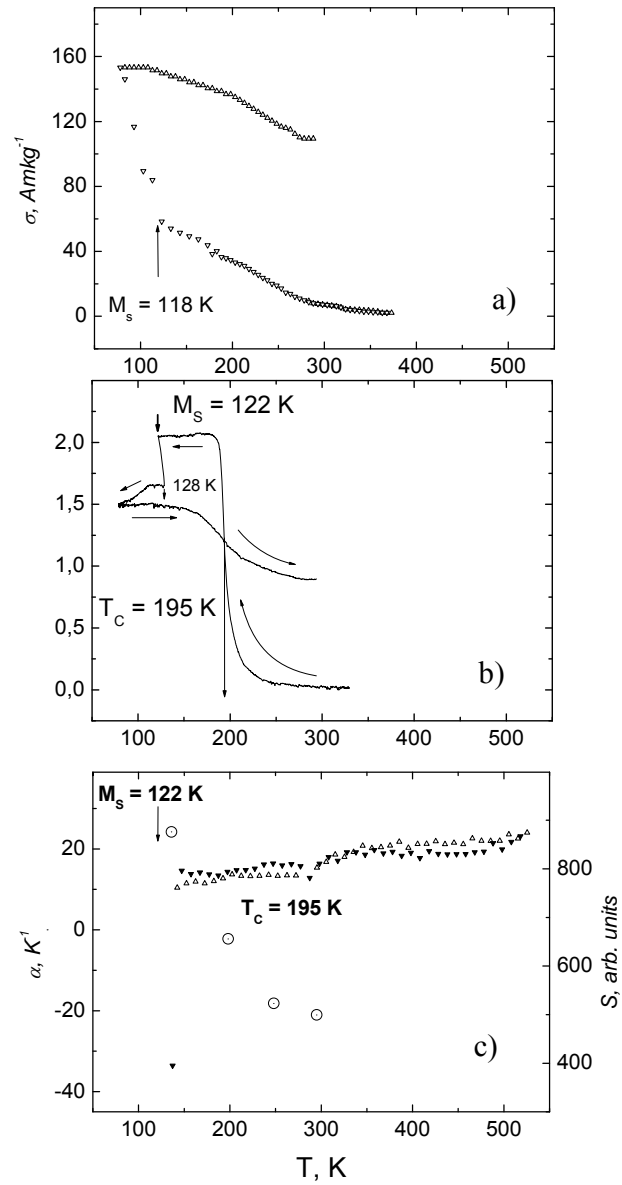


FIGURE 2. Saturation magnetization (a), magnetic susceptibility (b), TEC of Fe-25,3%Ni-0,73%C alloy and Mössbauer spectrum integral intensity (c) vs. temperature.

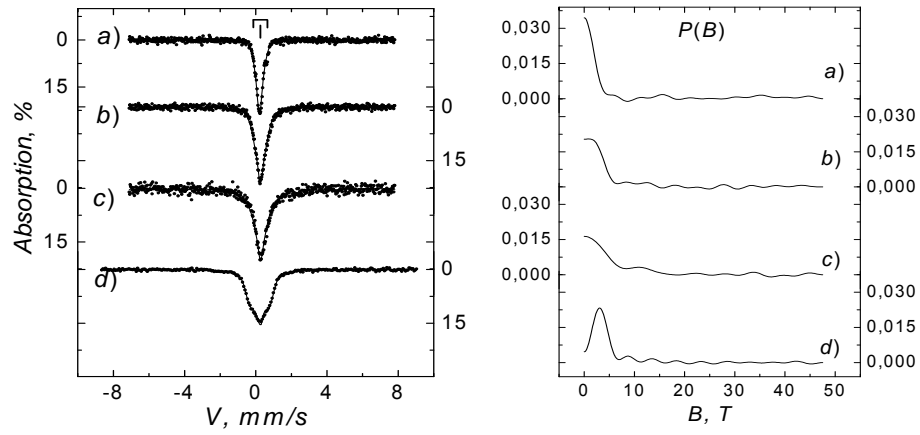


FIGURE 3. Mössbauer spectra and HMF distribution $p(B)$ of the Fe-25,3%Ni-0,73%C alloy derived at 295 K (a), 198 K (b), 163 K (c), and for the Fe-25,3%Ni-0,78%C alloy under external magnetic field 5 T (d).

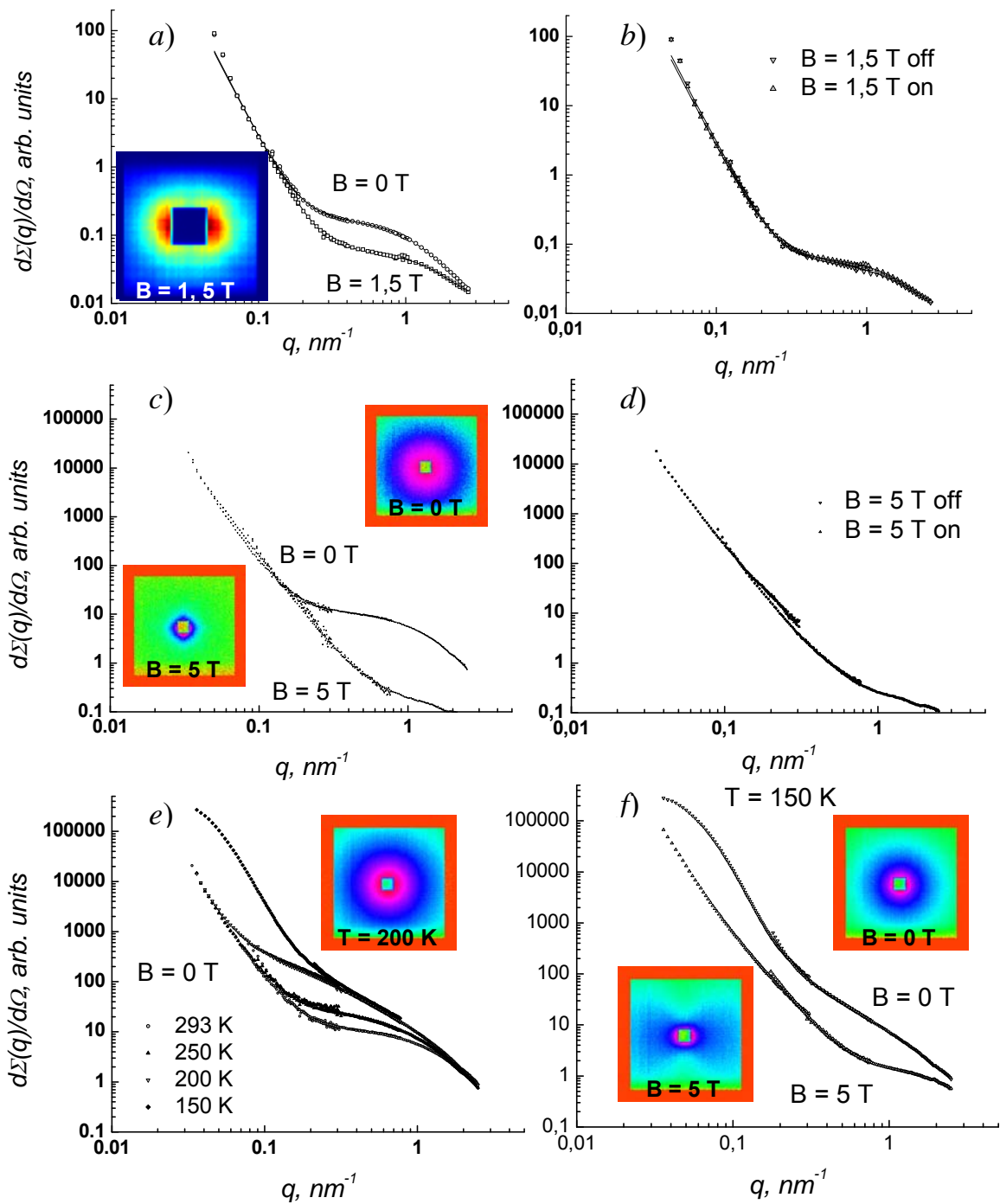


FIGURE 4. Results of SANS on the Fe-25,3%Ni-0,73%C alloy: SANS-1 in field 0 T and 1,5 T (a); SANS-1, polarised neutrons effect in field 1,5 T (b); SANS-2 in field 0 T and 5 T (c); SANS-2 polarised neutrons effect in field 5 T (d); SANS-2 at temperatures 293 K, 250 K, 200 K, 150 K (e); SANS-2 at temperature 150 K in field 0 T and 5 T. Colored squares appears to be smth like neutron flux cross-section at large q vectors.

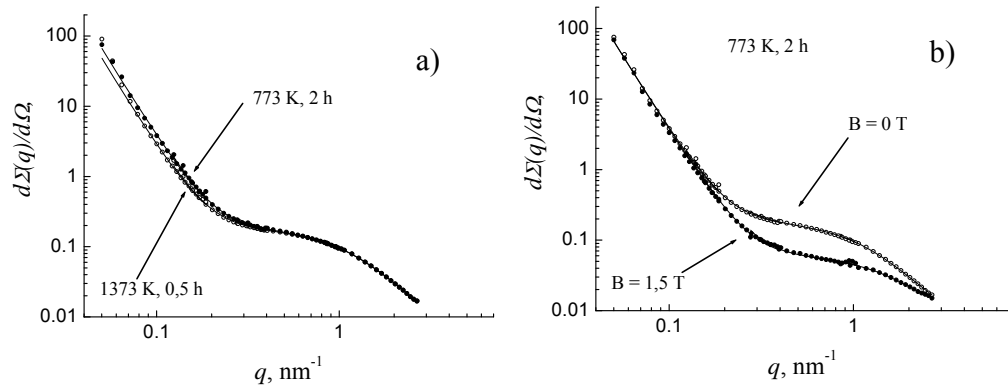


Figure 5. The φ -averaged and spin summarized SANS intensities in anti-Invar Fe–25.3%Ni–0.73%C (wt. %) alloy after annealing at 1373 K for 0,5 h and ageing at 773 K during 2 hrs (a); the effect of external magnetic field of 1,5 T (b).